

Supporting information

Hourglass-type Polyoxometalate-based Crystalline Materials as Efficient Cooperating Photocatalysts for the Reduction of Cr(VI) and Oxidation of Dye

Xuerui Tian, Yaqi Zhang, Yuanyuan Ma*, Qing Zhao and Zhangang Han*

Hebei Key Laboratory of Organic Functional Molecules; National Demonstration Center for Experimental Chemistry Education; College of Chemistry and Material Science, Hebei Normal University, Shijiazhuang, Hebei 050024, People's Republic of China

* Corresponding author. E-mail: mayy334@hebtu.edu.cn, hanzg116@126.com

List:

- 1. Supplementary Experimental Section**
- 2. Supplementary Figures**
- 2. Supplementary Tables**

1. Experimental Section

Standard curves of photocatalytic reduction of Cr(VI) and oxidation of MB

When the incident light, absorption coefficient and path length keep same, the transmitted light only changes with the concentration of the solution. So, in a certain range, the concentration c and absorbance A accord with the Lambert's law:

$$A = \kappa b c. \quad (1)$$

So its conversion rate can also be expressed as follows:

$$D = (A_0 - A_t) / A_0 \times 100\%. \quad (2)$$

Where D is the conversion, A_0 is the initial solution absorbance, and A_t is the solution absorbance at reaction time t (min).

Excess FA, if the reduction of Cr (VI) follows pseudo first-order kinetics, the rate constant k and reaction time t can be determined using the following equation:

$$\lg c_t (A) = \lg c_0 (A) - kt / 2.303 \quad (3)$$

The Arrhenius equation $k = Be^{-E_a/RT}$ is then changed into:

$$\lg k = -E_a/2.303RT + \lg B;$$

where

$$E_a = -19.15 \times k(\text{slope})$$

B is the pre-exponential factor, E_a is the apparent activation energy, and R and T are the gas constant and thermodynamic temperature (K), respectively.

2. Supplementary Figures

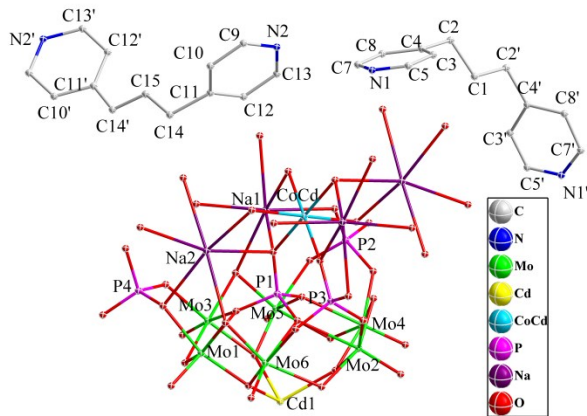


Fig. S1 Simplified diagram of the asymmetric unit of compound 1.

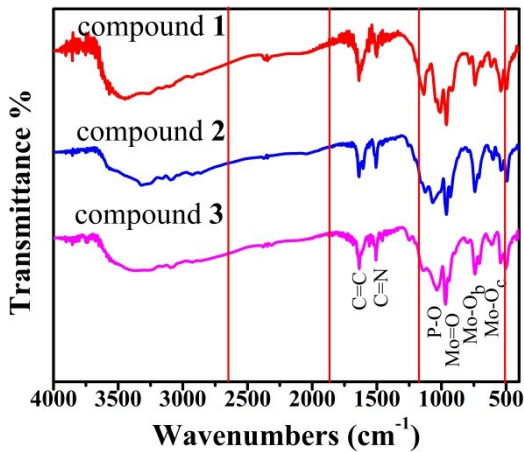


Fig. S2 IR spectra of 1-3 showing the different characteristic bands for polyanions and organic components.

IR spectra of compounds 1-3 were measured and exhibited the similar characteristic peaks at 4000-400 cm⁻¹ (Fig. S2). The peaks at 1015~1070 cm⁻¹ are attributed to anti-symmetric vibrations of $\nu_{as}(P-O_a)$. The $\nu(Mo=O_t)$ stretching vibration are in the vicinity of 960 cm⁻¹, and the strong peaks at 600~750 cm⁻¹ are ascribed to the characteristic absorption peak of $\nu(Mo-O)$ stretching vibration. The absorption peaks located near 1500~1600 cm⁻¹ are the stretching vibration of C=C and C=N bonds from the organic part of the three compounds. Furthermore, the broad peaks at 3250~3440 cm⁻¹ are assigned to the stretching vibration of $\nu(O-H)$, $\nu(C-H)$ and $\nu(N-H)$.

	Elements	Weight %	Atom %
Compound 1	C K	17.08	26.00
	O K	59.20	67.65
	P K	3.12	1.84
	Mo L	18.10	3.45
	Na K	0.89	0.71
	Cd L	1.04	0.17
	Co K	0.56	0.18
Sum		100.00	-
Compound 2	C K	36.62	48.64
	O K	47.98	47.84
	P K	2.76	1.42
	Mo L	11.77	1.96
	Cd L	0.72	0.10
	Zn K	0.15	0.04
	Sum	100.00	-
Compound 3	C K	23.83	38.99
	O K	41.63	51.14
	P K	5.79	3.67
	Mo L	25.60	5.24
	Cd L	2.44	0.43
	Al K	0.72	0.52
	Sum	100.00	-

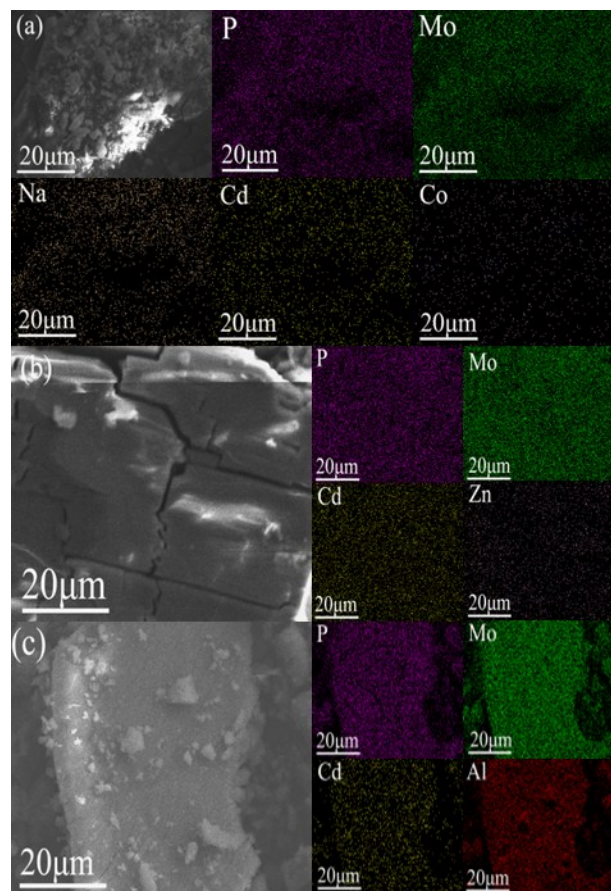


Fig. S3 EDS analysis results for representative elements in the relevant regions of compounds **1(a)**, **2(b)** and **3(c)**.

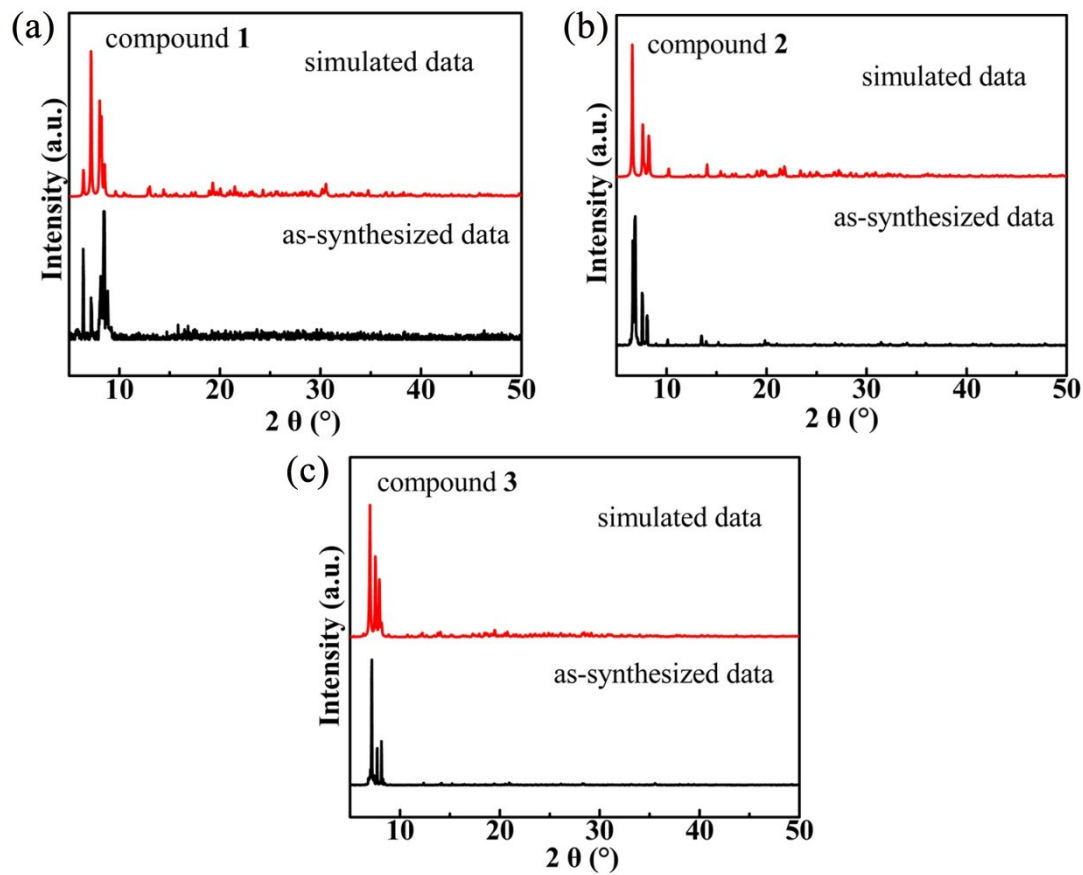


Fig. S4 The XRD patterns of compounds 1-3.

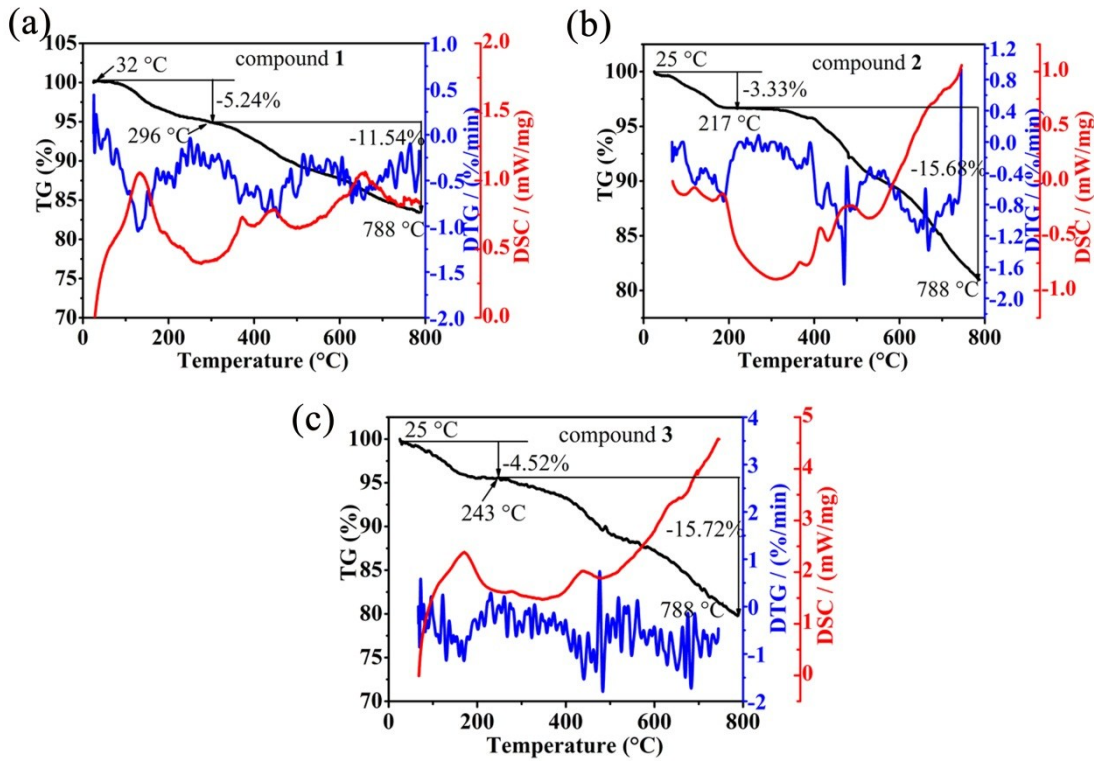


Fig. S5 TG, DTG and DSC curves for compounds **1-3**.

Thermogravimetric analysis of compounds **1-3** were carried out under a N₂ atmosphere from 20 to 800 °C. As seen from Fig. S5, TG curves of **1-3** exhibited the two weight-loss steps between 25 °C and 788 °C. Compound **1** has the actual weight loss of 5.24% (theoretical value 5.00%) in the range of 32-296 °C, which is equivalent to the loss of 2 crystal water and 7 coordination water molecules from metal Na/Cd/Co; the second step weight loss range at 296-788 °C, the actual weight loss is 15.54% (theoretical value 12.37%), which is equivalent to the loss of all protonated organic components. The TG-DSC curves of compound **2** showed that the weight loss from 25 °C to 217 °C is *ca.* 3.33% and is equivalent to the loss of lattice water (theoretical value: 3.22%), as the temperature rises to 788 °C, almost all of the protonated organic components are lost. At the same time, it can be seen from the figure that the inorganic frame structure remains intact even at very high temperatures. Similarly, for compound **3**, the overall weight loss is *ca.* 20.24% from 25 up to 788 °C, attributed to the loss of crystal waters and organic components (theoretical value: 19.54%).

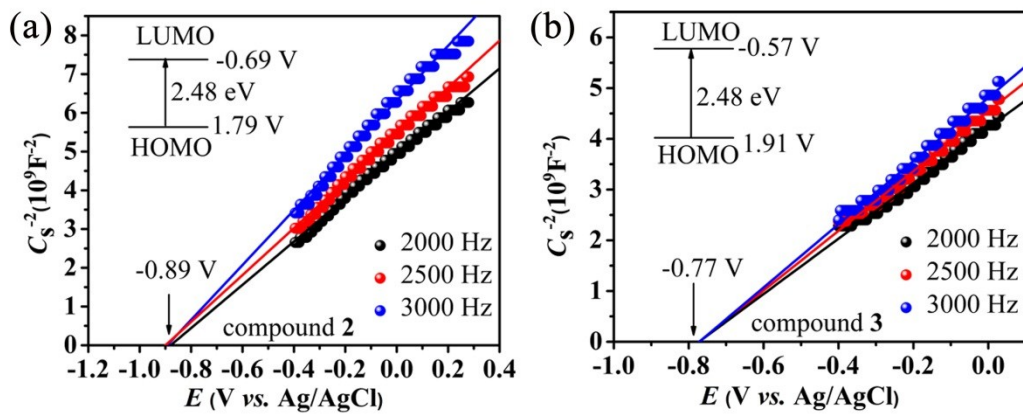


Fig. S6 Mott-Schottky plot of compounds **2-3** in 0.2 M Na_2SO_4 solution at pH = 6.80. Inset: Energy diagram of the HOMO and LUMO levels of **2-3**.

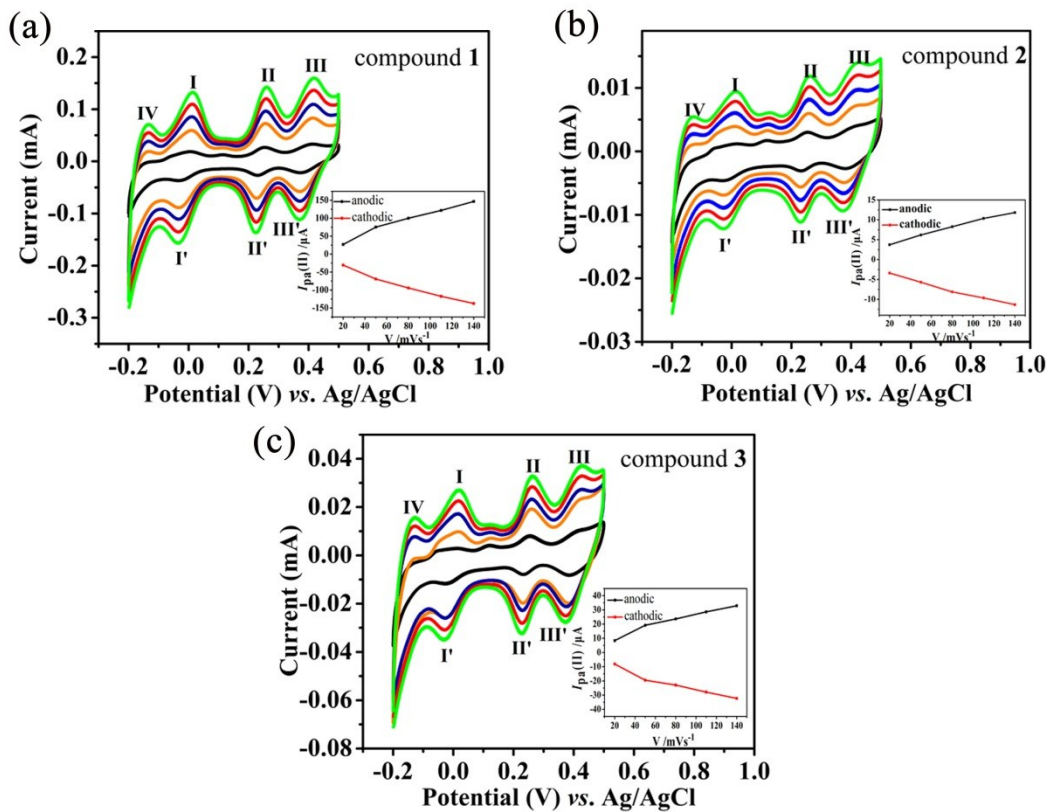


Fig. S7 Cyclic voltammograms of **1-3** with different sweep rates (20, 50, 80, 110, 140 mV·s⁻¹) in 1M H_2SO_4 solution. Inset is plot of peak current vs. scan rate for peak (I-I').

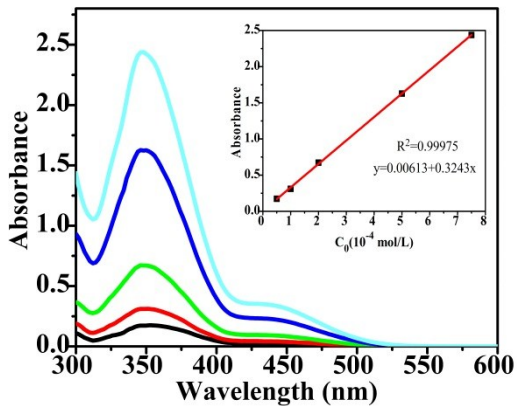


Fig. S8 UV absorption spectra of different concentrations of Cr(VI) solution (mass concentration from the inside out were 0.1×10^{-4} , 1×10^{-4} , 5×10^{-4} , 8×10^{-4} , 10×10^{-4} mol / L). The internal graph shows the relationship between the mass concentration of Cr(VI) solution and absorbance at a wavelength of 348 nm.

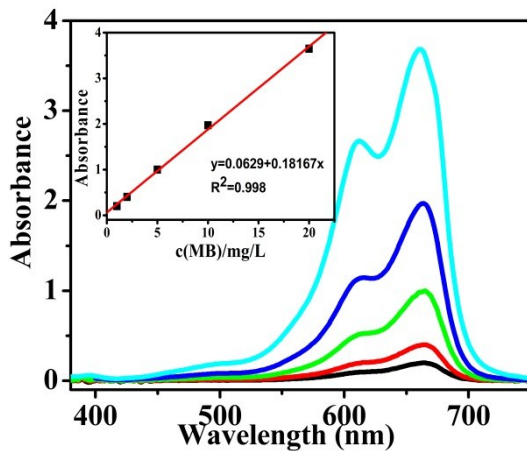


Fig. S9 UV absorption spectra of MB solutions with different mass concentrations (mass concentration is 1, 2, 5, 10, 20 mg/L from the inside out); internal plot is the mass concentration and absorbance of MB solution at 662 nm.

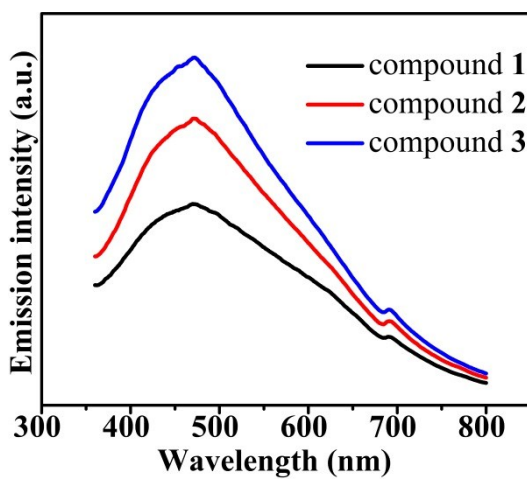


Fig. S10 Emission spectra of compounds **1-3** (solid) at room temperature.

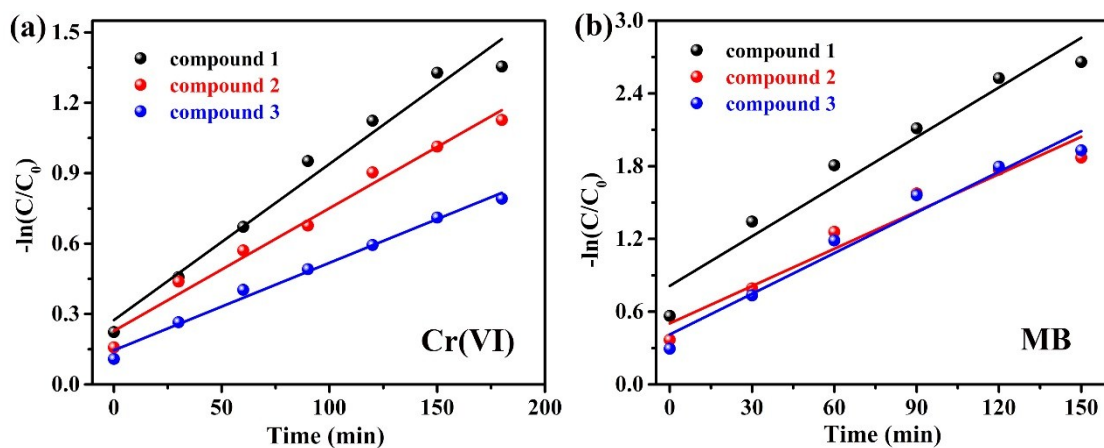


Fig. S11 The pseudo-first order kinetics plot for the photocatalytic reduction of Cr(VI) (a) and degradation of MB (b).

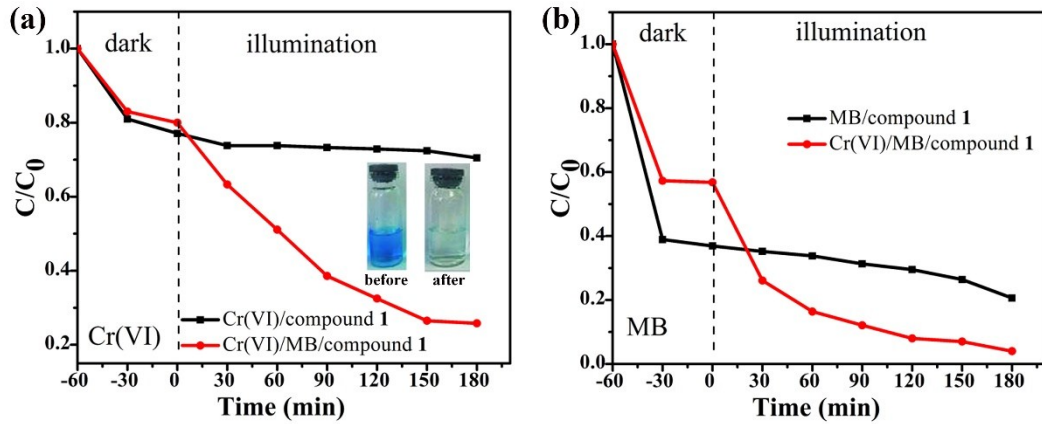


Fig. S12 Removals of (a) Cr(VI) or (b) MB in single or mixture solution over compound 1 photocatalyst under irradiation.

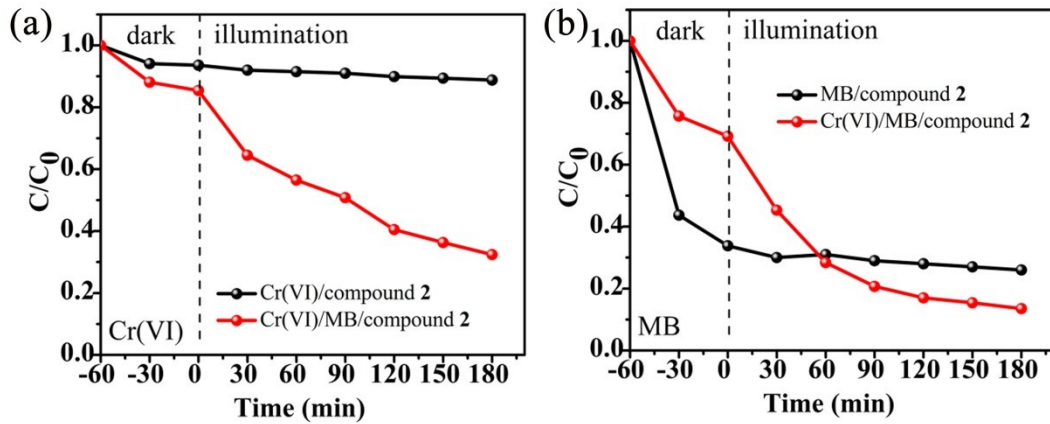


Fig. S13 Removals of (a) Cr(VI) or (b) MB in single or mixture solution over compound 2 photocatalyst under irradiation.

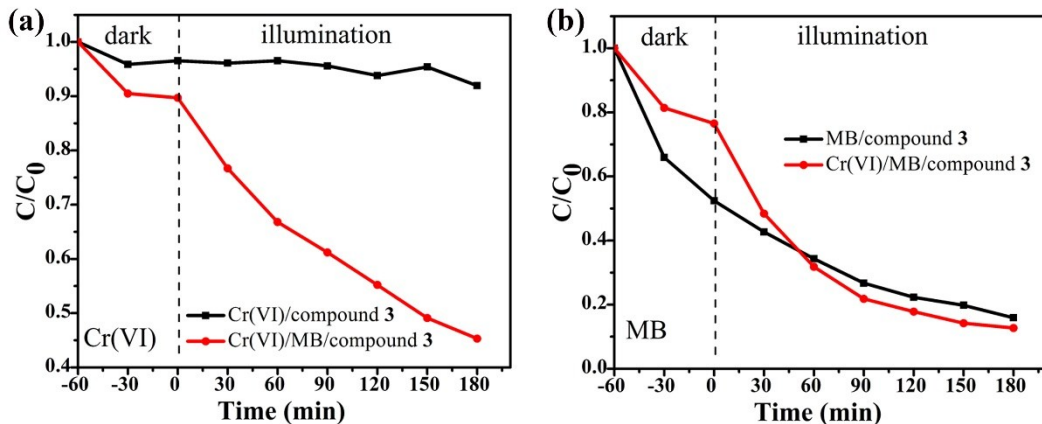


Fig. S14 Removals of (a) Cr(VI) or (b) MB in single or mixture solution over compound 3 photocatalyst under irradiation.

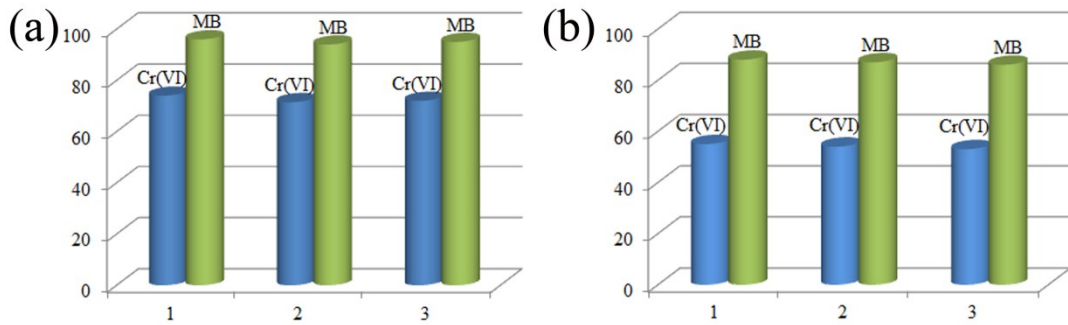


Fig. S15 Three parallel experiments of compound **1** (a) and **3** (b) photocatalyst under irradiation.

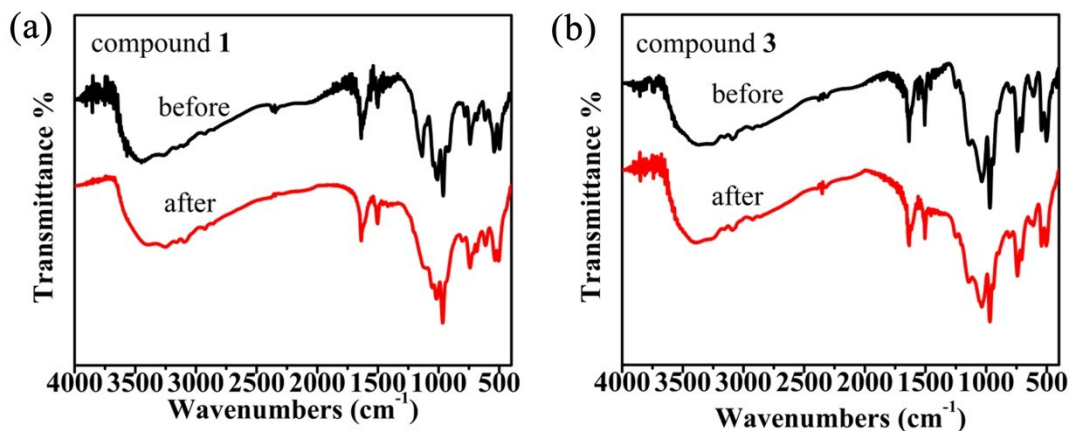


Fig. S16 Infrared spectra of compounds **1**, **3** before and after catalytic experiments. The slight shift of the absorption peak of $3250\text{-}3440\text{ cm}^{-1}$ may stem from the reason that the catalyst is not completely air-dried after catalysis.

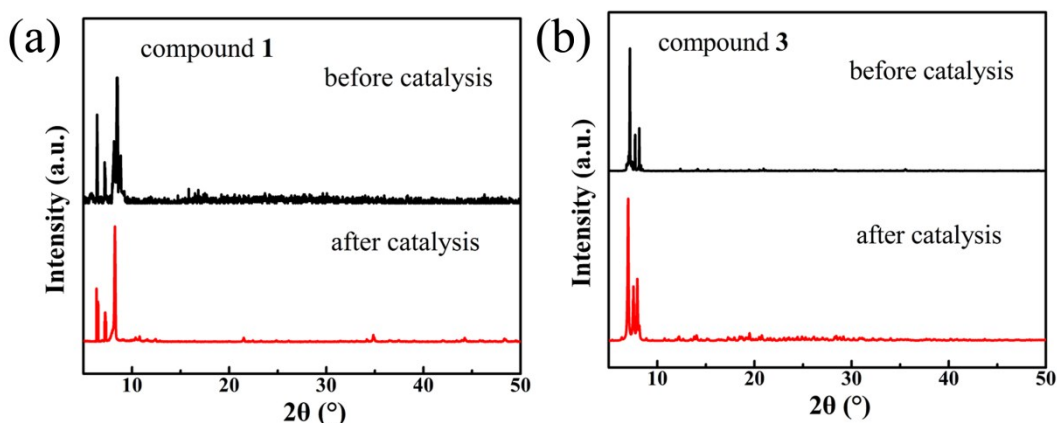


Fig. S17 The XRD of compounds **1**, **3** before and after catalytic experiments.

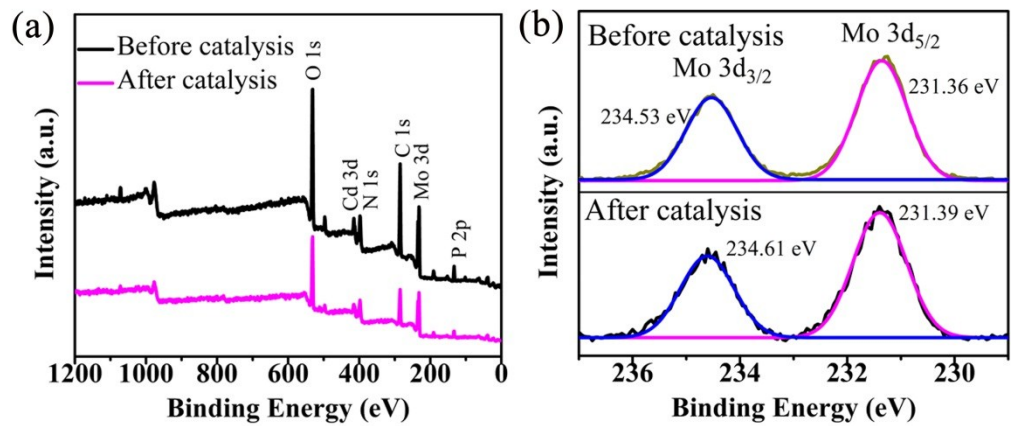


Fig. S18 XPS spectra of compound 2: (a) the full survey; (b) Mo 3d XPS of before and after the reaction.

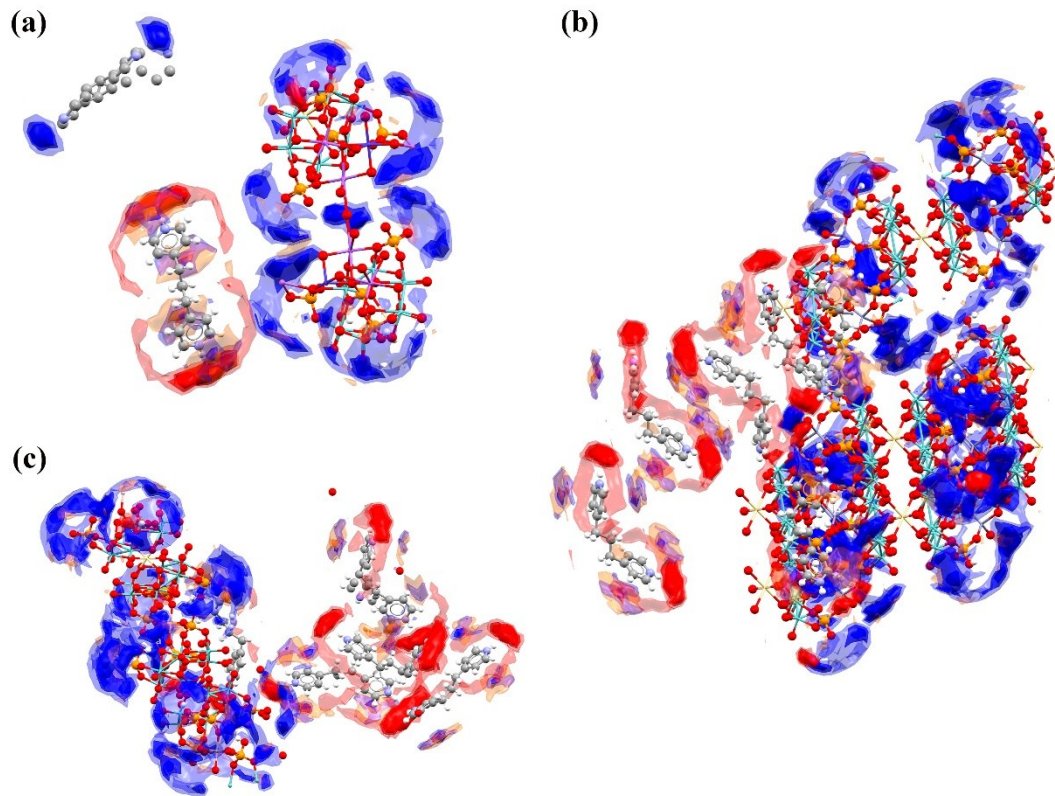


Fig. S19 The interaction map of compounds 1-3. The blue area represents the position that can absorb positive charged species and the red area represents the sites that can absorb negative charged species.

3. Supplementary Tables

Table S1. Crystal data and structure refinement details for compounds **1-3**.

Compound	1	2	3
Formula	C ₂₆ H ₆₀ Cd _{1.20} Co _{0.80} Mo ₁₂ N ₄ Na ₄ O ₇₁ P ₈	C ₃₉ H ₇₂ CdMo ₁₂ N ₆ O ₆₈ P ₈ Zn ₂	C ₆₅ H ₁₁₀ Al ₂ Cd ₂ Mo ₂₄ N ₁₀ O ₁₃ ₇ P ₁₆
Mr.	3237.8	3355.25	6300.47
Cryst. Syst.	Monoclinic	Triclinic	Monoclinic
Space group	<i>C</i> 2/ <i>c</i>	<i>P</i> -1	<i>P</i> n
<i>a</i> (Å)	21.0842(6)	13.126(4)	15.8820(18)
<i>b</i> (Å)	18.3743(5)	25.198(7)	21.676(2)
<i>c</i> (Å)	21.9022(6)	30.034(8)	25.338(3)
α, β, γ (°)	90, 100.716(3), 90	113.698(4), 101.194(4), 90.634(4)	90, 94.559(2), 90
Volume (Å ³), <i>Z</i>	8337.1(4), 4	8879(4), 4	8695.4(17), 2
<i>D</i> _{cal} (Mg·m ⁻³)	2.582	2.510	2.409
μ (mm ⁻¹)	2.492	2.658	2.182
<i>F</i> ₍₀₀₀₎	6241	6496	6084
Crystal size (mm ³)	0.17 × 0.15 × 0.13	0.19 × 0.17 × 0.15	0.17 × 0.15 × 0.13
θ (°)	3.129 to 25.010	2.074 to 25.010	1.738 to 25.010
Reflections collected	15730	39555	39054
Independent Refl.	7315 [<i>R</i> _(int) = 0.0255]	29329 [<i>R</i> _(int) = 0.0261]	19835 [<i>R</i> _(int) = 0.0256]
Max and min. tran.	0.723 and 0.661	0.671 and 0.610	0.753 and 0.697
Data/restraints/parameter	7315 / 643 / 623	29329 / 1369 / 2437	19835 / 1673 / 2317
GOF on <i>F</i> ²	1.044	1.049	1.057
<i>R</i> ₁ , <i>wR</i> ₂ [<i>I</i> >2σ(<i>I</i>)]	<i>R</i> ₁ = 0.0423, <i>wR</i> ₂ = 0.1122	<i>R</i> ₁ =0.0468, 0.1188	<i>R</i> ₁ = 0.0334, <i>wR</i> ₂ = 0.0883
<i>R</i> ₁ , <i>wR</i> ₂ (all data)	<i>R</i> ₁ = 0.0488, <i>wR</i> ₂ = 0.1173	<i>R</i> ₁ = 0.0661, 0.1312	<i>R</i> ₁ = 0.0374, <i>wR</i> ₂ = 0.0925

Table S2. Selected bond lengths (\AA) and bond angles ($^{\circ}$) of compound **1**.

Mo(1)-O(27)	1.677(5)	Mo(5)-O(21)	1.680(5)	P(2)-O(14)	1.534(5)
Mo(1)-O(8)	1.937(5)	Mo(5)-O(19)	1.927(5)	P(2)-O(10)	1.550(5)
Mo(2)-O(9)	1.675(5)	Mo(6)-O(15)	1.676(5)	P(3)-O(30)	1.576(5)
Mo(2)-O(3)	1.935(5)	Mo(6)-O(8)	1.925(5)	P(4)-O(25)	1.494(6)
Mo(3)-O(22)	1.679(5)	Cd(1)-O(11)	2.196(5)	Na(1)-O(17)	2.425(7)
Mo(3)-O(19)	1.939(5)	Cd(1)-O(6)	2.198(4)	Na(1)-O(1)	2.460(6)
Mo(4)-O(10)	2.079(5)	P(1)-O(20)	1.541(5)	Na(2)-O(4W)	2.727(7)
Mo(4)-O(7)	2.124(5)	P(1)-O(13)	1.551(5)	O(30)-Na(1)#2	2.528(7)
O(2)-Mo(1)-O(26)	158.3(2)	O(15)-Mo(6)-O(8)	106.4(2)	Na(1)-P(1)-Na(2)	78.26(5)
O(27)-Mo(1)-O(8)	106.5(2)	O(8)-Mo(6)-O(2)	95.2(2)	O(17)-P(2)-O(10)	111.7(3)
O(9)-Mo(2)-O(6)	101.4(2)	O(2)-Cd(1)-O(2)#1	180.0	O(31)-P(3)-O(29)	113.1(3)
O(22)-Mo(3)-O(11)	100.3(2)	Na(2)-Cd(2)-Na(2)#2	180.0	O(25)-P(4)-O(23)	112.9(3)
O(16)-Mo(4)-O(6)	102.4(2)	P(2)-Na(1)-Cd(2)	97.37(8)	P(1)-O(20)-Mo(1)	127.2(3)
O(3)-Mo(4)-O(6)	95.3(2)	O(26)-Na(2)-O(1)	106.2(3)	Mo(1)-O(26)-Na(2)	100.3(2)
O(21)-Mo(5)-O(11)	102.9(2)	O(1)-Na(2)-O(3w)	96.5(4)	P(3)-O(29)-Mo(2)	130.1(3)
O(19)-Mo(5)-O(11)	95.8(2)	O(1w)-Na(2)-O(4w)	97.5(4)	P(3)-O(31)-Cd(2)	156.1(3)

Symmetry transformations used to generate equivalent atoms: #1 $-x+3/2, -y+3/2, -z+2$; #2 $-x+2, -y+1, -z+2$

Table S3. Selected bond lengths (\AA) and bond angles ($^\circ$) of compound **2**.

Mo(1)-O(1)	1.687(6)	Mo(8)-O(42)	1.677(6)	Mo(24)-O(103)	2.292(5)
Mo(1)-O(3)	1.951(5)	Mo(8)-O(43)	1.945(5)	P(1)-O(23)	1.544(5)
Mo(2)-O(3)	1.958(5)	Mo(10)-O(57)	1.688(6)	P(4)-O(32)	1.582(6)
Mo(2)-O(2)	1.969(5)	Mo(10)-O(60)	1.954(5)	P(5)-O(37)	1.542(5)
Mo(3)-O(17)	1.688(6)	Mo(11)-O(49)	1.695(5)	P(6)-O(30)	1.591(6)
Mo(3)-O(21)	1.937(5)	Mo(11)-O(45)	1.954(5)	P(7)-O(38)	1.524(5)
Mo(4)-O(21)	1.936(5)	Mo(13)-O(63)	1.703(5)	P(10)-O(85)	1.574(6)
Mo(4)-O(15)	1.978(5)	Mo(14)-O(76)	2.285(5)	P(11)-O(68)	1.512(6)
Mo(5)-O(27)	1.707(5)	Mo(15)-O(90)	1.682(6)	P(12)-O(82)	1.571(6)
Mo(5)-O(26)	1.938(5)	Mo(16)-O(77)	2.315(5)	P(13)-O(110)	1.535(5)
Mo(6)-O(26)	1.959(5)	Mo(19)-O(94)	1.701(5)	P(16)-O(121)	1.568(6)
Mo(6)-O(12)	1.986(5)	Mo(20)-O(105)	2.337(5)	Cd(1)-O(15)	2.279(5)
Mo(7)-O(50)	1.704(6)	Mo(21)-O(117)	1.697(5)	Cd(2)-O(55)	2.270(5)
Mo(7)-O(43)	1.932(5)	Mo(22)-O(109)	2.320(5)	Cd(3)-O(72)	2.313(5)
Zn(1)-O(18)	1.943(5)	Zn(3)-O(79)	1.949(5)	Zn(4)-O(110)	1.946(5)
Zn(2)-O(37)	161.7(4)	Zn(3)-O(97)	1.951(6)	Zn(4)-O(87) ^{#1}	1.957(5)
O(1)-Mo(1)-O(3)	106.9(3)	O(44)-Mo(12)-Mo(1)	88.68(1)	O(51)-P(5)-O(52)	107.6(3)
O(6)-Mo(2)-O(2)	102.5(3)	O(90)-Mo(15)-O(84)	105.7(3)	O(59)-P(8)-O(61)	111.4(3)
O(17)-Mo(3)-O(21)	106.2(3)	O(77)-Mo(16)-Mo(5)	88.13(1)	O(71)-P(9)-O(7)	107.6(3)
O(11)-Mo(6)-O(12)	101.4(2)	O(106)-Mo(23)-O(1)	180.0	O(120)-P(16)-O(122)	109.4(3)
O(50)-Mo(7)-O(43)	108.3(3)	O(13)-Mo(24)-Mo(3)	180.0(3)	O(15)-Cd(1)-O(15) ^{#2}	180.0
O(44)-Mo(8)-Mo(7)	88.75(12)	O(23)-P(1)-O(16)	106.7(8)	O(55) ^{#3} -Cd(2)-O(55)	180.0
O(58)-Mo(9)-O(60)	106.5(3)	O(7)-P(2)-O(13)	109.0(3)	O(73) ^{#4} -Cd(3)-O(73)	180.0(3)
O(38)-Zn(2)-O(37)	116.4(2)	O(68)-Zn(3)-O(97)	102.0(3)	O(83)-Zn(4)-O(111)	96.5(2)

Symmetry transformations used to generate equivalent atoms: #1 $x-1, y, z$; #2 $-x+2, -y+1, -z+1$; #3 $-x+1, -y, -z+1$; #4 $-x+1, -y+1, -z+2$

Table S4. Selected bond lengths (\AA) and bond angles ($^\circ$) of compound **3**.

Mo(1)-O(54)	1.669(9)	Mo(15)-O(108)	2.085(8)	P(4)-O(102)	1.517(9)
Mo(2)-O(19)	1.945(9)	Mo(18)-O(80)	1.682(10)	P(6)-O(109)	1.495(9)
Mo(3)-O(72)	1.670(9)	Mo(19)-O(37)	2.229(9)	P(7)-O(37)	1.563(9)
Mo(4)-O(101)	1.938(9)	Mo(22)-O(28)	1.970(9)	P(9)-O(121)	1.529(10)
Mo(5)-O(48)	1.691(10)	Mo(23)-O(35)	2.278(9)	P(10)-O(43)	1.498(9)
Mo(6)-O(95)	1.925(9)	Cd(1)-O(9)	2.256(9)	P(11)-O(90)	1.547(12)
Mo(7)-O(36)	1.672(10)	Cd(2)-O(28)	2.254(8)	P(12)-O(52)	1.483(11)
Mo(8)-O(95)	1.918(8)	Al(2)-O(40)	1.862(9)	P(13)-O(71)	1.536(11)
Mo(9)-Mo(19)	2.6190(17)	P(1)-O(26)	1.701(5)	P(14)-O(119)	1.468(13)
Mo(10)-O(65)	1.671(10)	P(1)-O(96)	2.337(5)	P(14)-O(123)	1.486(15)
Mo(11)-Mo(18)	2.5901(14)	P(2)-O(56)	1.475(10)	P(15)-O(55)	1.474(9)
Mo(12)-O(116)	1.683(10)	P(2)-O(59)	1.523(10)	P(15)-O(67)	1.516(10)
Mo(13)-Mo(14)	2.5973(17)	P(3)-O(60)	1.495(11)	P(16)-O(40)	1.509(8)
Mo(14)-O(122)	1.665(10)	P(3)-O(92)	1.506(11)	P(16)-O(21)	1.515(8)
O(54)-Mo(1)-O(101)	105.1(5)	O(5)-Mo(14)-Mo(13)	86.4(2)	O(6)-P(1)-O(96)	113.9(5)
O(53)-Mo(2)-O(20)	102.2(5)	O(76)-Mo(17)-O(29)	170.0(4)	O(6)-P(2)-O(58)	114.8(6)
O(72)-Mo(3)-O(104)	106.2(5)	O(1)-Mo(18)-Mo(11)	88.5(2)	O(6)-P(3)-O(92)	109.3(7)
O(44)-Mo(4)-O(3)	102.1(5)	O(9)-Mo(21)-O(17)	107.0(5)	O(2)-P(4)-O(25)	107.9(5)
O(48)-Mo(5)-O(111)	104.4(5)	O(5)-Mo(22)-Mo(20)	87.7(2)	O(1)-P(5)-O(73)	104.9(5)
O(114)-Mo(6)-O(9)	101.6(4)	O(10)-Cd(1)-O(9)	179.8(4)	O(3)-P(8)-O(14)	110.1(7)
O(37)-Mo(7)-Mo(21)	88.4(2)	O(7)-Cd(1)-O(3)	179.7(4)	O(6)-P(9)-O(70)	111.0(6)
O(118)-Mo(8)-O(95)	106.5(5)	O(28)-Cd(2)-O(27)	178.9(4)	O(9)-P(10)-O(9)	104.2(6)
O(33)-Mo(12)-O(8)	95.4(4)	O(34)-Al(2)-O(55)	94.1(5)	O(6)-P(15)-O(9)	106.9(5)
O(63)-Mo(13)-O(5)	94.4(5)	O(34)-Al(2)-O(40)	97.3(4)	O(4)-P(1)-O(21)	112.7(5)

Table S5. BVS calculations of Mo, P and M centers in compounds **1-3**.

	Mo1	Mo2	Mo3	Mo4	Mo5	Mo6	P1	P2	P3	P4	Cd1	Cd2
1	5.220	5.257	5.220	5.252	5.286	5.268	4.866	4.845	4.856	4.815	2.661	2.314
	Mo1	Mo2	Mo3	Mo4	Mo5	Mo6	Mo7	Mo8	Mo9	Mo10	Mo11	Mo12
	5.025	5.052	5.036	5.019	4.926	5.071	4.981	5.064	4.975	5.068	4.997	5.024
	Mo13	Mo14	Mo15	Mo16	Mo17	Mo18	Mo19	Mo20	Mo21	Mo22	Mo23	Mo24
2	5.002	4.958	5.092	5.044	5.035	5.116	4.980	5.119	4.995	5.052	5.070	5.037
	P1	P2	P3	P4	P5	P6	P7	P8	P9	P10	P11	P12
	4.623	4.736	4.651	4.790	4.601	4.757	4.694	4.745	4.618	4.717	4.692	4.814
	P13	P14	P15	P16	Cd1	Cd2	Cd3	Cd4	Zn1	Zn2	Zn3	Zn4
	4.581	4.777	4.717	4.736	2.141	2.123	2.131	2.146	2.052	2.012	2.094	2.022
	Mo1	Mo2	Mo3	Mo4	Mo5	Mo6	Mo7	Mo8	Mo9	Mo10	Mo11	Mo12
	5.344	5.308	5.344	5.295	5.221	5.407	5.271	5.429	5.351	5.294	5.282	5.351
3	P1	P2	P3	P4	P5	P6	P7	P8	P9	P10	P11	P12
	4.918	4.915	5.048	4.908	4.985	4.905	4.849	4.885	4.888	4.981	4.885	5.213
	P13	P14	P15	P16	Cd1	Cd2	Al1	Al2				
	4.817	5.334	5.044	5.959	2.300	2.237	3.189	3.204				

Table S6. Selected hydrogen bonding lengths and angles for compound **1**.

Donor-H...Acceptor	D-H [Å]	H...A [Å]	D...A [Å]	D-H...A [°]
N(1)-H(1)...O(7 ⁱ)	0.86	1.98	2.780(11)	154
O(5)-H(5D)...O(6 ⁱⁱ)	0.94	1.89	2.810(7)	163
O(7)-H(7D)...O(2 ⁱⁱ)	0.83	1.92	2.742(8)	169
O(12)-H(12D)...O(2)	0.75	2.56	2.800(6)	101
O(12)-H(12D)...O(6)	0.75	2.52	2.803(7)	105
O(12)-H(12D)...O(11 ⁱⁱ)	0.75	2.08	2.829(6)	177
O(18)-H(18)...N(2 ⁱⁱⁱ)	0.82	2.57	3.164(19)	131
O(18)-H(18)...N(2 ^{iv})	0.82	2.22	2.99(2)	156
O(24)-H(24)...N(3w)	0.82	2.45	3.224(17)	157
C(3)-H(3)...O(22 ^v)	0.93	2.29	3.162(12)	156

Symmetry codes: i = 1-x,y,3/2-z; ii = 3/2-x,3/2-y,2-z; iii = 1-x,1-y,2-z; iv = 1/2+x,-1/2+y,z; v = 1-x,1-y,1-z.

Table S7. Selected hydrogen bonding lengths and angles for compound 2.

Donor-H...Acceptor	D-H [Å]	H...A [Å]	D...A [Å]	D-H...A [°]
N(1)-H(1A)...O(54 ⁱ)	0.86	2.30	2.938(14)	131
N(2)-H(2A)...O(65 ⁱⁱ)	0.86	2.02	2.840(10)	159
N(3)-H(3)...O(5 ⁱⁱⁱ)	0.86	2.01	2.791(10)	150
N(4)-H(4A)...O(93 ^{iv})	0.86	2.12	2.875(15)	146
N(5)-H(5A)...O(114 ^v)	0.86	2.05	2.806(12)	145
N(7)-H(7)...O(41)	0.86	2.04	2.831(11)	153
N(9)-H(9A)...O(75 ^{vi})	0.86	2.10	2.940(12)	167
N(11)-H(11)...O(37)	0.86	2.16	2.991(12)	162
O(13)-H(13)...O(53 ^{vii})	0.82	2.10	2.834(8)	149
O(32)-H(32)...O(23)	0.82	2.28	2.989(9)	145
C(4)-H(4)...O(56 ^{iv})	0.93	2.49	3.272(12)	141
C(12)-H(12)...O(57 ^{iv})	0.93	2.41	3.234(11)	147
C(17)-H(17)...O(101 ^{viii})	0.93	2.32	3.137(11)	146
C(22)-H(22)...O(94 ^v)	0.93	2.49	3.410(16)	169
C(53)-H(53)...O(74 ^{vi})	0.93	2.37	3.178(15)	146

Symmetry codes: i = -1+x, 1+y, z; ii = 1-x, 1-y, 1-z; iii = 2-x, 1-y, 1-z; iv = x, 1+y, z; v = -x, 1-y, 2-z;

vi = -1+x, y, z; vii = 1+x, y, z; viii = 1+x, 1+y, z.

Table S8. Selected hydrogen bonding lengths and angles for compound 3.

Donor-H...Acceptor	D-H [Å]	H...A [Å]	D...A [Å]	D-H...A [°]
N(1)-H(1A)...O(60 ⁱ)	0.86	2.08	2.86(2)	151
N(5)-H(5A)...O(5 ⁱⁱ)	0.86	1.92	2.748(17)	161
N(6)-H(6)...O(1 ⁱⁱⁱ)	0.86	1.95	2.766(19)	158
N(9)-H(9A)...O(33 ^{iv})	0.86	1.88	2.730(15)	169
O(47)-H(47)...O(84)	0.82	1.88	2.618(13)	149
O(75)-H(75)...O(30)	0.82	2.37	2.972(14)	130
O(99)-H(99)...O(19)	0.82	1.89	2.634(13)	151
C(22)-H(22)...O(4 ^v)	0.93	2.46	3.31(3)	152
C(27)-H(27)...O(72 ⁱⁱ)	0.93	2.33	3.20(2)	156
C(39)-H(39)...O(77 ⁱⁱⁱ)	0.93	2.32	3.14(2)	146
C(53)-H(53)...O(92 ^{iv})	0.93	2.03	2.93(2)	161

Symmetry codes: i = x, -1+y, z; ii = -1/2+x, 1-y, -1/2+z; iii = x, y, -1+z; iv = x, -1+y, -1+z; v = 1/2+x, 1-y, -1/2+z.

Table S9. Peak potential data (mV) for each peak of compounds **1-3** at a sweep speed of $140 \text{ mV}\cdot\text{s}^{-1}$.

Scan rate 140 mV s^{-1}	$Ea/Ec \text{ (I) / mV}$ $E_{1/2}, \Delta E$	$Ea/Ec \text{ (II) / mV}$ $E_{1/2}, \Delta E$	$Ea/Ec \text{ (III) / mV}$ $E_{1/2}, \Delta E$	$Ea/Ec \text{ (IV) / mV}$
Compound 1	15 / -35 -10, 50	261 / 223 242, 38	415 / 368 392, 47	-133
Compound 2	8 / -28 -10, 36	260 / 229 245, 31	420 / 369 395, 51	-129
Compound 3	16 / -30 -7, 46	262 / 227 245, 35	427 / 373 400, 54	-130

Table S10. Comparison of pollutant removal with various other reported POM-based materials.

catalyst	time (min)	pollutants	light source	conversion (%)	ref
Crystal 1	180	Cr(VI)-MB	visible	74%-96%	This work
[Cu ₄ (μ ₃ -OH) ₂ (H ₂ O) ₆ (4-dpye) ₂ (TeMo ₆ O ₂₄)] <cdot2h<sub>2O</cdot2h<sub>	90	MB	UV	73%	1
[Cd ₃ (2,3'-Htmbpt) ₂ (2,3'-tmbpt) ₄ (γ-Mo ₈ O ₂₆)(β-Mo ₈ O ₂₆)(H ₂ O) ₄] <cdot5h<sub>2O</cdot5h<sub>	120	MB	UV	56%	2
[Ag(phen) ₂] ₂ (Agphen) ₂ SiW ₁₂ O ₄₀	210	MB	UV	70%	3
PPy@Ag ₂₉ SiW ₁₂	360	RhB	UV	48%	4
WO ₃ _x /NC	90	VOC	visible	92%	5
[Ag ₄ (H ₂ O)(L) ₃ (SiW ₁₂ O ₄₀)]	160	Cr(VI)	visible	99%	6
Ag/Ag _x H _{3-x} PMo ₁₂ O ₄₀	40	Cr(VI)	visible	68%	7
PMo ₁₂ /TiO ₂ /Ag-X	60	Cr(VI)	visible	71%	8
SiW ₁₂ O ₄₀ H ₄	600	Cr(VI)-RhB	visible	75%-99%	9

Table S11. The summary of Zeta potential of the reported POM-based complexes.

POM-based complexes	Zeta potential/ ζ mV	pH	ref
[α-PW ₁₁ O ₃₉ Fe ^{III}] ⁴⁻ -O - -ligated hematite-core complex	-40±5	8	10
{[Cu(H ₂ biim) ₂][{Cu(H ₂ biim) ₂ (H ₂ O) ₂ Cu ₂ biim}(H ₂ O) ₂]-H[({Cu(H ₂ biim)(H ₂ O) ₂ } _{0.5}) ₂ ((C ₃ HN ₂ Cl ₂) {Cu(H ₂ biim)} ₂) _n]}{Na(H ₂ O)P ₅ W ₃₀ O ₁₁₀ }]·xH ₂ O	-30	3.5-8.5	11

P2W18/MIL-101(Cr)	-12.5	-	12
[PBI] ₅ Ru ₄ POM	-39.9	8	13
CitNPs@POV	-49.6±1.7		14
C ₁₆ IPS/Mo ₇	-40	-	15

References:

- [1] X. L. Wang, J. J. Sun, H. Y. Lin, Z. H. Chang, X. Bai and X. Wang, Polyhedron, 2017, **124**, 30-40.
- [2] W. Q. Kan, S. Z. Wen, Y. H. Kan, H. Y. Hu, S. Y. Niu and X. Y. Zhang, Synthetic Met., 2014, **198**, 51-58.
- [3] H. J. Pang, Y. Niu, J. Yu, H. Y. Ma, Q. F. Song and S. B. Li, Inorg. Chem. Commun., 2015, **59**, 5-8.
- [4] J. Q. Sha, X. Y. Yang, N. Sheng, G. D. Liu, J. S. Li and J. B. Yang, J. Solid State Chem., 2018, **263**, 52-59.
- [5] L. Y. Wang, X. X. Xu, S. J. Wu and F. Cao, Catal. Sci. Technol., 2018, **8**, 1366-1374.
- [6] H. Zhang, J. Yang, Y. Y. Liu, S. Y. Song, X. L. Liu and J. F. Ma, Dyes Pigments, 2016, **133**, 189-200.
- [7] H. F. Shi, G. Yan, Y. Zhang, H. Q. Tan, W. Z. Zhou, Y. Y. Ma, Y. G. Li, W. L. Chen and E. B. Wang, ACS Appl. Mater. Inter., 2017, **9**, 422-430.
- [8] S. Kim, J. Yeo and W. Choi, Appl. Catal. B: Environ., 2008, **84**, 148-155.
- [9] H. F. Shi, Y. C. Yu, Y. Zhang, X. J. Feng, X. Y. Zhao, H. Q. Tan, S. U. Khan, Y. G. Li and E. B. Wang, Appl. Catal. B, 2018, 221, 280-289
- [10] B. Chakraborty, G. Gan-Or, Y. Duan, M. Raula, I. A. Weinstock, Angew. Chem. Int. Ed., 2019, 58, 6584-6589.
- [11] J. Du, M. D. Cao, S. L. Feng, F. Su, X. J. Sang, L. C. Zhang, W. S. You, M. Yang, Z. M. Zhu, Chem. Eur. J. 2017, 23, 14614 – 14622.
- [12] A. Jarrah, S. Farhadi, Acta Chim. Slov., 2019, 66, 85–102.
- [13] M. Bochino, Z. Syrgiannis, M. Burian, N. Marino, E. Pizzolato, K. Dirian, F. Rigodanza, G. A. Volpato, G. Ganga, N. Demitri, S. Berardi, H. Amenitsch, D. M. Guldi, S. Caramori, C. A. Bignozzi, A. Sartorel, M. Prato, Nat. Chem., 2019, 11, 146–153.
- [14] S. Tomane, E. Lopez-Maya, S. Boujday, V. Humblot, J. Marrot, N. Rabasso, J. Castells-Gil, C. Sicard, A. Dolbecq, P. Mialane, A. Vallee, Nanoscale Adv., 2019, 1, 3400-3405.
- [15] N. Sun, A. L. Wu, Y. Yu, X. P. Gao, L. Q. Zheng, Chem. Eur. J. 2019, 25, 6203-6211.